Dynamic Behaviors of Silt and Sandy Silt Soils Determined from Cyclic Ring Shear Tests

Ali El Takch

Hatch Engineering, Niagara Falls, ON, Canada

Abouzar Sadrekarimi, and Hesham El Naggar

Department of Civil & Environmental Eng. – Western University, London, ON, Canada

ABSTRACT

Despite the large volume of experimental studies on the dynamic behavior of sands and silty sands, the dynamic undrained characteristics of cohesionless silts and sandy silts are less understood. A comprehensive laboratory testing program is conducted to characterize the dynamic properties of silt and sandy silt soils with 75% and 50% silt contents. The elastic soil behavior at very small shear strains ($\gamma < 10^{-4}$%) is investigated through shear wave velocity (V_s) measurements using bender elements at vertical stresses ranging from 50 to 300 kPa. In addition, strain-controlled constant-volume cyclic ring shear tests are carried out to establish shear modulus (G) and damping ratio (D) at larger shear strain amplitudes ($\gamma > 0.01$%) and investigate the influence of silt content and γ on these parameters. The results demonstrate that V_s and the maximum shear modulus (G_o) increase with increasing silt content. V_s is also found to vary with the effective overburden stress to the power of 0.31 - 0.34 for all silt and sandy silt mixes. The results further show that while undrained G decreases with increasing γ, D increases with increasing γ only up to $\gamma < 1$%, beyond which it exhibits a decreasing trend.

1 INTRODUCTION

Shear wave velocity, V_s (also called S-wave or secondary wave velocity) is an important parameter used in many geotechnical earthquake engineering applications, including evaluation of soil liquefaction resistance using empirical relationships (Andrus, et al., 1999; Youd, et al., 2001) and design of foundations subjected to dynamic loads (El Naggar, 2003). As a shear wave produces negligible slippage at particle contacts, it propagates primarily by the elastic deformation of particles at their contacts. Shear wave velocity thus represents soil elasticity and provides a direct measure of the maximum (small-strain) shear stiffness (G_o) of a soil as below:

$$G_o = \rho V_s^2 \tag{1}$$

where G_o is in Pa, V_s is in m/s, and ρ is the total soil mass density in kg/m^3. Along with soil damping characteristics, G_o is a useful parameter for analysis of natural or man-made structures under dynamic or cyclic loads (e.g., caused by an earthquake, machine foundation, ocean waves, or blast).

With increasing shear strain (> 0.001%), soil particles start to slip at their contacts and even rearrange in addition to their elastic deformation. This results in soil stiffness degradation, which is determined by a secant shear modulus (G) or a reduction of the normalized shear modulus, G/G_o (Matasovic and Vucetic, 1995). G is obtained from the slope of the line connecting the tips of a cyclic stress-strain loop as illustrated in Figure 1 and using the following equation:

$$G = \frac{\tau_{max} - \tau_{min}}{\gamma_{max} - \gamma_{min}} \tag{2}$$

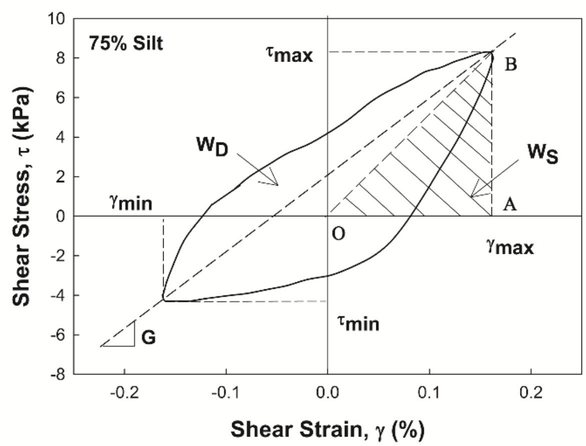

Figure 1: A cyclic stress-strain loop from a constant-volume cyclic ring shear test on a specimen with 75% silt content at $\gamma = 0.16$% and $\sigma'_{vc} = 100$ kPa

The damping ratio (D) of soils represents the energy dissipated in a soil element during a cycle of loading by friction among soil particle, particle rearrangement, and soil non-linear behavior. This is determined as below:

$$D = \frac{W_D}{4\pi W_S} \quad (3)$$

where W_D is the energy dissipated in one cycle of loading, calculated from the area of the hysteresis cyclic loop, and W_S is the maximum strain energy stored during the loading cycle, equal to the triangular area of OAB in Figure 1. Shear modulus reduction and damping ratio of saturated soils are essential for predicting strain level, and carrying out seismic ground response and soil structure interaction analyses.

Cyclic triaxial testing is commonly used for determining G/G_o and D of cohesionless soils (El Mohtar, et al., 2013, Georgiannou, et al., 1991, Wichtmann, et al., 2015). A soil specimen in a cyclic triaxial test experiences: 1) typically isotropic consolidation, 2) repeated 90º flipping of principal stresses from compression to extension, 3) axisymmetric boundary conditions, and 4) possible necking during extension loading. These characteristics differ from field stress conditions which are seldom isotropic and involve a smooth rotation of principal stresses often under plane-strain boundary conditions. These discrepancies make it difficult and complicated to directly apply cyclic triaxial test results to field conditions.

In this study, a comprehensive laboratory testing program is carried out using an advanced cyclic ring shear testing apparatus in order to characterize the elastic and cyclic behaviors of silts and sandy silts (with fines contents more than 50%). Cyclic ring shear testing essentially resembles a direct simple shear test, in which a soil specimen is consolidated under zero-lateral strain (K_o) and then subjected to a plane-strain simple shearing mode with smooth and continuous cyclic rotation of principal stresses. These characteristics provide a closer replicate of field boundary conditions and shearing mode of in-situ soils.

2 SPECIMEN PREPARATION

Reconstituted specimens of non-plastic silt and sandy silts with 50% and 75% silt content (SC) were prepared and tested in this study. The silt (MIN-U-SIL 40) was obtained from US Silica Company (Berkeley Springs, West Virginia), and it was mainly composed of white-colored quartz particles. Scanning electron microscopic images of the silt particles indicated angular and irregular particle shapes. The added sand was a quartz Ottawa sand with round to sub-rounded particle shapes. Table 1 presents the index properties of the tested materials. The coating of sand particles with finer silt particles is a natural phenomenon for silty sands and sandy silts, which produces a bulking effect in a moist-tamped soil structure. Because of this bulking behavior, the ASTM (2006a, 2006b) standard methods were not applicable for the soils of this study, and therefore we determined the maximum (e_{max}) and minimum (e_{min}) void ratios using a slurry deposition technique (Bradshaw and Baxter, 2007) and the modified proctor procedure (ASTM, 2012), respectively. We found that e_{max} and e_{min} and their difference increased with increasing silt content as shown in Table 1, which is consistent with those reported by other investigators (Naeini and Baziar, 2004, Yamamuro and Covert, 2001).

Table 1. Index properties of the soils used in this study

Soil	Silt	Sandy silt	Sandy silt	Ottawa sand
SC (%)	100	75	50	0
D_{50} (mm)	0.012	0.029	0.070	0.450
e_{max}	2.09	1.48	1.15	0.74
e_{min}	0.67	0.58	0.46	0.42
C_u	10.28	5.40	7.80	1.38
C_c	1.84	0.82	0.63	1.00

Note: C_u and C_c are coefficients of uniformity and curvature, respectively.

The moist tamping method was used to prepare all specimens of this study. Water and air pluviation methods were avoided because of the potential segregation of silt and sand particles leading to non-uniform samples (Carraro and Prezzi, 2008; Kuerbis and Vaid, 1988; Wang, et al., 2011). In particular, due to low permeability, mechanical vibration would be ineffective for densifying silt samples prepared by water pluviation or slurry deposition.

For preparing moist-tamped specimens, dry soil was mixed at 5% moisture content and subsequently poured and tamped in 3 layers into the specimen mold. The under-compaction technique (Ladd, 1978) was also followed in order to produce uniform specimens by accounting for the increased density of the lower layers induced by compacting the upper sand layers. This technique has been demonstrated to provide cyclic shear strength in silts comparable to that of undisturbed samples recovered by in-situ ground freezing (Bradshaw and Baxter, 2007). The method is also quick, easy, and ensures that the compaction effort is distributed evenly throughout a specimen.

3 EFFECT OF SOIL MOISTURE

Because of the low permeability of silt and sandy silt specimens of this study, non-uniform pore pressure could develop during shearing if the samples were saturated (Zhou, et al., 1995). Therefore, in order to avoid complexities associated with the effect and the measurement of local pore water pressure, the ring shear tests were carried out without sample saturation. However, the small moisture content of 5% used for moist tamping could develop suction among the silt and sand particles and produce an increases in effective stress and soil shear resistance (Lu, et al., 2007). The amount of soil suction was thus examined using an auxiliary suction control and measurement panel of the cyclic ring shear apparatus. This panel included dual air pressure regulators with fine and coarse gauges for the measurement of matric suction. We measured matric suctions of 100 – 120 kPa in the moist-tamped specimens. Because of the very low saturation ratio (8 – 15%) of our moist-tamped specimens, the effective stress parameter which describes the contribution of matric suction to soil effective stress was about 0.05 (Lu and Likos, 2004). Accordingly, soil suction among the moist sand and silt particles merely added a maximum of about 5 to 6 kPa to σ'_{vc}. This rather small increase in σ'_{vc} is accounted for in the results and interpretations of shear modulus and damping ratio of this study.

4 SHEAR WAVE VELOCITY MEASUREMENT

Cyclic constant-volume ring shear tests and shear wave velocity readings were conducted at the soil mechanics laboratory of Western University using an advanced ring shear testing apparatus (SRS-150) manufactured by GCTS (Arizona, United States). In this apparatus, an annular specimen of up to 30 mm high is confined between inner and outer solid confining rings with inner (R_i) and outer (R_o) radii of 48.3 mm and 76.1 mm, respectively. This provides an effective specimen area of 108.8 cm^2. The ratio of the inner to outer radii is 0.63, which conforms to the ASTM (2006c) recommendations for ring shear testing. In this study, V_s was measured after the application of the consolidation vertical stress (σ'_{vc}) using a pair of piezoelectric bender elements embedded in the upper and lower platens of the ring shear specimen chamber. V_s was calculated from the travel time (t) of an electrical pulse and the tip-to-tip distance (d_{sr}) between the transmitter and receiver bender elements. For the specimens of this study, we observed that most of the signal received by the bender element was transmitted at frequencies less than 75 kHz. Accordingly, a low-pass filter with a cut-off frequency of 75 kHz was applied to the transmitted signals to eliminate electrical noise. As shown in Figure 2, a consistent and clear shear wave response was obtained.

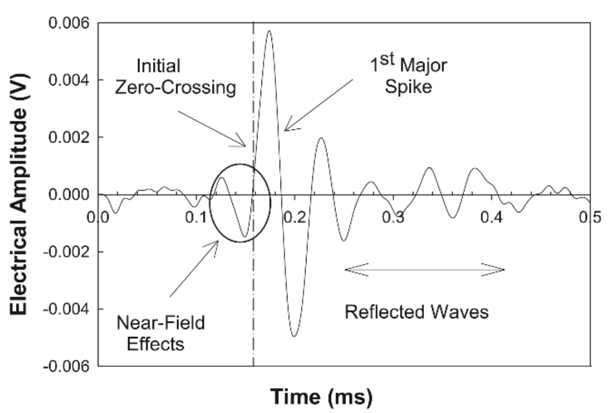

Figure 2: Typical electrical signal received by a bender element and the interpretation of shear wave arrival time in this study for a pure silt specimen at D_{rc} = 35% and σ'_{vc} = 100 kPa

Although the measurement of d_{sr} was relatively straightforward and precise, detecting the arrival time of the first shear wave could be challenging and uncertain. Several studies suggest that the initial zero-crossing time of the first major signal provides a reasonable estimate of V_s for silts and sands (Baxter, et al., 2008; Kawaguchi, et al., 2001; Lee and Santamarina, 2005). Accordingly, as illustrated in Figure 2, the time of the initial zero-crossing of the first major electrical signal captured by the receiving bender element was selected here for determining the propagation time. V_s was measured at σ'_{vc} ranging from 50 to 300 kPa, in 50 kPa increments. Figure 3 presents the variations of V_s over this range of σ'_{vc} for the specimens of this study.

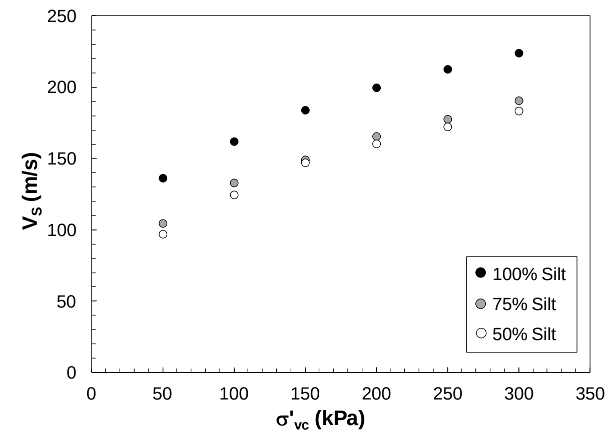

Figure 3: Shear wave velocity versus σ'_{vc} (= 50 - 300 kPa) for pure silt and sandy silt specimens

5 CYCLIC RING SHEAR TESTING AND RESULTS

In order to investigate the cyclic behaviour of silts and sandy silts at large strains (γ > 0.01%), series of strain-controlled constant-volume cyclic ring shear tests were carried out. In these experiments, the shearing force (T) is applied through a ring-shaped platen at the specimen's top, while the solid confining rings and the bottom platen remained stationary. The surfaces of the platens in contact with the soil are indented with radial grooves in order to prevent slippage and effectively transfer the shearing load to the specimen. An advanced computer-controlled electro-pneumatic servo motor applies vertical (σ_v) and shear (τ) stresses of up to 1,000 kPa and 1,300 kPa, respectively at a rate of 0.001º/min to 360º/min on the specimen. The normal force (N) and the shearing torque (T) applied on the specimen are measured with a combined force-torque transducer. The average shear and effective vertical stresses on a horizontal failure plane within the specimen are calculated using the following relationships (ASTM, 2006c; La Gatta, 1970):

$$\tau = \frac{3T}{2\pi\left(R_o^3 - R_i^3\right)} \tag{4}$$

$$\sigma_v = \frac{N}{\pi\left(R_o^2 - R_i^2\right)} \tag{5}$$

The average shear displacement (δ) and shear strain (γ) at the mid-radius of the specimen are also calculated as below:

$$\delta = \frac{\pi}{180}\left(\frac{R_o+R_i}{2}\right)\theta \quad (6)$$

$$\gamma = \frac{\delta}{h} \quad (7)$$

In which θ is the magnitude of the rotational twist (in degrees) applied in the ring shear tests. The ring shear specimens of this study were first consolidated to $\sigma'_{vc} = 100$ kPa and then they were subjected to a sinusoidal cyclic shear stress at a frequency of 0.1 Hz with shear stress reversal. As the dynamic shearing response (e.g., fast earthquake excitation) of saturated cohesionless soils is generally regarded as undrained, several studies have investigated shear modulus reduction and damping ratio using either element-scale laboratory tests carried out under undrained or constant-volume cyclic shearing conditions (Alarcon-Guzman, et al., 1989; El Mohtar, et al., 2013; Lanzo, et al., 1997; Sitharam, et al., 2015) or dynamic centrifuge modeling (El Gamal, et al., 2005; Stevens, 2001) experiments. Undrained shearing is also recommended by the ASTM (2011) standard procedure for determining modulus and damping properties of soils. Undrained shearing was thus replicated in the cyclic ring shear tests by a constant-volume condition. The variation of vertical stress during constant-volume cyclic shearing is regarded as an equivalent pore-water pressure change that would develop in a truly undrained test (ASTM, 2007; Dyvik, et al., 1987; Sadrekarimi and Olson, 2009).

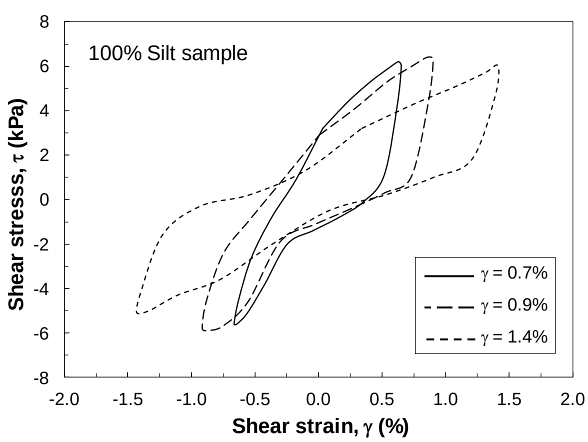

Figure 4: Cyclic stress-strain response of a silt specimen in a constant-volume cyclic ring shear test at $\gamma = 0.7\%$, 0.9%, and 1.4%

A constant volume was maintained during shearing by continuously adjusting the vertical stress applied on the soil specimen. This was carried out by a precise LVDT feedback and vertical stress control system in the ring shear apparatus. Figure 4 shows a typical example of the stress-strain loops at different strain levels for a soil specimen with 75% silt content. As illustrated in Figure 4, the stress-strain loops became more slender and formed an S-shape with increasing γ. This change in the shape of the cyclic stress-strain loops reflects significant changes in stiffness and damping behavior of the silt and sandy silt specimens which are discussed in the following paragraphs.

6 DISCUSSION

The results of the bender element measurements and cyclic ring shear tests are subsequently combined in order to characterize soil behavior at a wider range of shear strain (γ). The former are used to evaluate the elastic soil behavior at very small shear strains ($\gamma < 10^{-4}\%$) and the latter are employed to characterize the plastic soil behavior at larger shear strains ($\gamma > 0.01\%$).

6.1 Elastic soil behavior at very small shear strains ($\gamma < 10^{-4}\%$)

Small strain behavior of the specimens is characterized by V_s measured using bender elements and G_o calculated from Equation (1). Figure 5 presents the variations of G_o for the silt and sandy silt specimens versus their consolidation void ratios (e_c). According to this figure, G_o sharply decreases with increasing e_c for all specimens, which indicates the significant effect of e_c on G_o (Alarcon-Guzman, et al., 1989). At a certain e_c, G_o also increases with increasing silt content, particularly from silty sand to pure silt specimens. Both phenomena can be explained by the increasing number of particle contacts (as e_c decreases or silt content increases), and hence the shear wave is transmitted through a larger number of particles resulting in higher V_s and G_o.

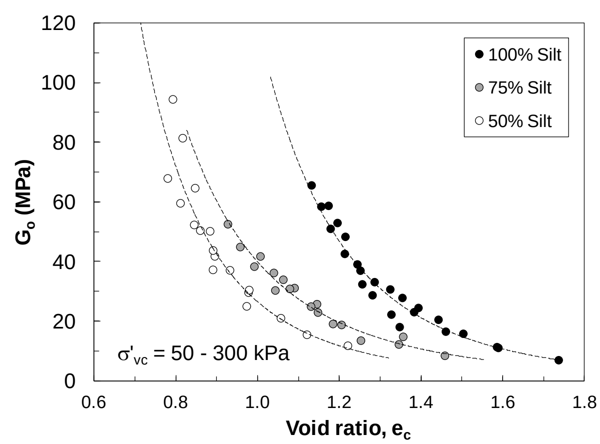

Figure 5: Effect of e_c and silt content on G_o

A general relationship between e_c and G_o for normally-consolidated soils is provided below (Kramer, 1996):

$$\frac{G_o}{p_a} = 625F(e_c)\left(\frac{\sigma'_m}{p_a}\right)^n \quad (8)$$

In which F(e$_c$) is a function of e$_c$, n is a stress exponent (often taken as 0.5 for sandy soils), σ'_m is the effective mean stress, and P$_a$ is the atmospheric pressure (≈ 100 kPa) with the same unit as σ'_m and G$_o$. For the normally-consolidated specimens of this study, σ'_m is calculated as $(1+2K_o)\sigma'_{vc}/3$. Based on an average friction angle (ϕ') of 35^o for the specimens of this study (El Takch, 2013), $K_o = 1 - \sin(\phi') = 0.42$ is assumed here (Mesri and Hayat, 1993). Several forms of empirical correlations have been proposed in the literature for F(e$_c$), some of which are summarized below:

Richart Jr. et al. (1970): $F(e_c) = \frac{(2.973-e_c)^2}{1+e_c}$ (9)

Hardin (1978): $F(e_c) = \frac{1}{0.3+0.7e_c^2}$ (10)

Jamiolkowski (1991): $F(e_c) = \frac{1}{e_c^{1.3}}$ (11)

Figure 6 presents the normalized maximum shear modulus, $G_o/625(\sigma'_m)^{0.5}$ and e$_c$ from the measurements of this study. Despite the similar trends of normalized shear moduli with e$_c$ for silt contents of 50% and 75%, the greater number of particle contacts produces higher $G_o/625(\sigma'_m)^{0.5}$ in pure silt specimens.

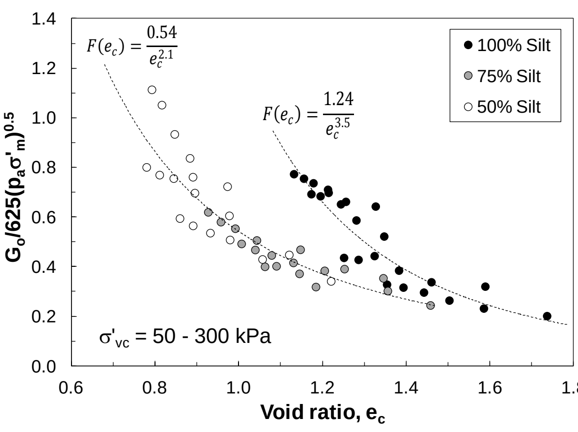

Figure 6: Variations of normalized maximum shear modulus ($G_o/625(p_a\sigma'_m)^{0.5}$) with e$_c$ for the silt and sandy silt specimens of this study

According to Figure 6, the following F(e$_c$) are curve-fitted for the pure silt and sandy silt specimens of this study:

For pure silt: $F(e_c) = \frac{0.54}{e_c^{2.1}}$ (12)

For sandy silts (FC = 75% and 50%): $F(e_c) = \frac{1.24}{e_c^{3.5}}$ (13)

These correlations can be used in Equation (8) for predicting G$_o$ of silts and sandy silts. In simplified liquefaction analysis based on shear wave velocity, the effect of overburden stress is accounted for by normalizing V$_s$ at σ'_{vc} = 100 kPa (V$_{s1}$). The measured V$_s$ at different magnitudes of σ'_{vc} are employed here to examine stress normalization of V$_s$ for the silt and sandy silt soils of this study. As illustrated in Figure 7, the variation of V$_{s1}$/V$_s$ with σ'_{vc} can be described by the following power function:

$$\frac{V_{s1}}{V_s} = \left(\frac{P_a}{\sigma'_{vc}}\right)^{\alpha} \quad (14)$$

In which, the stress exponent (α) varies from 0.33 to 0.38 for the silt and sandy silt specimens of this study. This (α = 0.33 – 0.38) is greater than α = 0.25 suggested by Robertson et al. (1992).

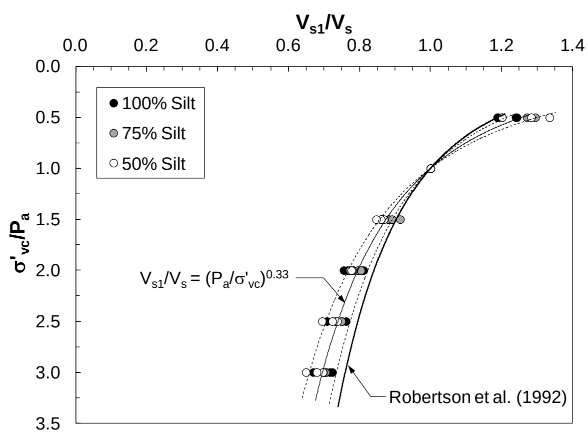

Figure 7: Relationships between normalized shear wave velocity (V$_{s1}$) and σ'_{vc} for the silt and sandy silt specimens of this study

7 SOIL CYCLIC BEHAVIOR AT LARGE SHEAR STRAINS (γ > 0.01%)

Constant-volume cyclic ring shear tests were carried out to determine secant shear modulus (G) and damping ratio (D) of the soil samples at large strains (γ > 0.01%). The variations of G and D with γ are described below.

7.1 Shear modulus at large strains ($\gamma > 0.01\%$)

As illustrated in Figure 4, the slope of the stress-strain loops and thus G progressively decrease with increasing the number of loading cycles and γ. The reduction of soil stiffness with γ is represented by the shear modulus reduction curves (G/G_o) in Figure 8. Since these relationships are determined from constant-volume ring shear tests, they are applicable to dynamic loads producing an undrained shearing condition (e.g., fast dynamic excitation during an earthquake).

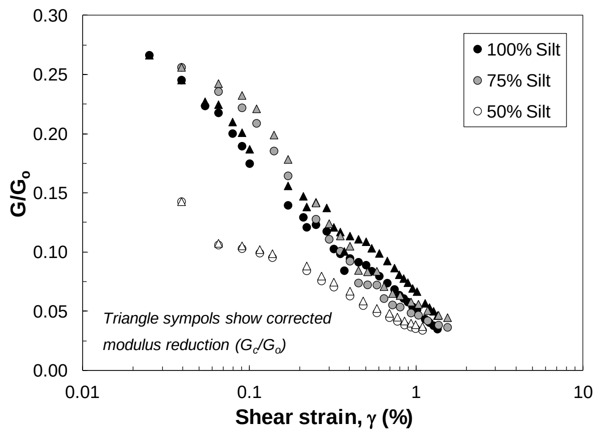

Figure 8: Shear modulus reduction curves for pure silt and sandy silt specimens at σ'_{vc} = 100 kPa

Therefore, besides increasing soil non-linear behavior at large strains, G/G_o reduction may have also resulted from the decrease in effective vertical stress (σ'_v) during constant-volume shearing. In order to examine the effect of σ'_v reduction, the modulus reduction data obtained from the cyclic ring shear tests are corrected based on the following relationship suggested by El Mohtar et al. (2013):

$$G_c = G\left(\frac{\sigma'_{vc}}{\sigma'_v}\right)^n \quad (15)$$

In which, G_c is the undrained shear modulus corrected for the effect of σ'_v reduction and n is a stress exponent similar to Equation (8). As demonstrated in Figure 8, the corrected modulus reduction data (G_c/G_o) are very close to the original G/G_o.
Previous experimental studies using resonant column and torsional shear tests (Assimaki, et al., 2000; Laird and Stokoe, 1993) also indicate the negligible effect of σ'_v changes at σ'_v < 110 kPa on modulus reduction and damping ratio of cohesionless soils. These evidences support the trivial effect of σ'_v reduction on the dynamic characteristics of the silt and sandy silt specimens determined from the constant-volume cyclic ring shear tests of this study. Furthermore, according to Figure 8 at any given cyclic strain level the amount of stiffness reduction is greater for specimens with 50% silt content, while those for the higher silt contents are practically the same. It is possible that the sand particles created greater disparity in the sandy silt fabric (at 50% silt content) which enhanced its compressibility and resulted in a larger modulus reduction.

7.2 Cyclic damping ratio at large strains ($\gamma > 0.01\%$)

Figure 9 presents the damping ratio (calculated using Eq. 3) versus γ for the specimens of this study. All specimens initially exhibit a small-strain ($\gamma < 0.1\%$) damping ratio of about 0.8 – 1.2%. With increasing shear strain, the amount of energy dissipated in each loading cycle rises as the friction among soil particles is mobilized. This is manifested in the cyclic ring shear test results as an increase of the area of the cyclic stress-strain loop (W_D) in Figure 4 (from γ = 0.7% to 0.9%) and hence soil damping ratio in Figure 9. Similar observations (increasing D with γ) are made by many other investigators (Vucetic, et al., 1998; Zhang, et al., 2005). However, as the cyclic shear strain amplitude approaches 1%, the damping ratios decrease. As illustrated in Figure 4 for a pure silt specimen, the area of the cyclic stress-strain loop initially grows (from γ = 0.7% to 0.9%), but then it becomes narrower (from γ = 0.9% to 1.4%), resulting in a reduced dissipated energy and damping ratio. Extensive review of the available literature shows that previous studies of soil dynamic behavior have often investigated damping ratios for strain levels of only up to 1%, whereas this peculiar behavior occurs at $\gamma \geq 0.9$ – 1.0%. Although we have not carried out further investigation regarding the particle-level mechanism of this phenomenon, localization of shear strain and dilation at high strain levels ($\gamma \geq 1\%$) are plausible mechanisms. Reduced damping at large shear strains have been also reported in some undrained direct simple shear tests on sands (Matasovic and Vucetic, 1993; Vucetic, 1986), as well as in centrifuge model experiments on saturated Nevada sand (El Gamal, et al., 2005).

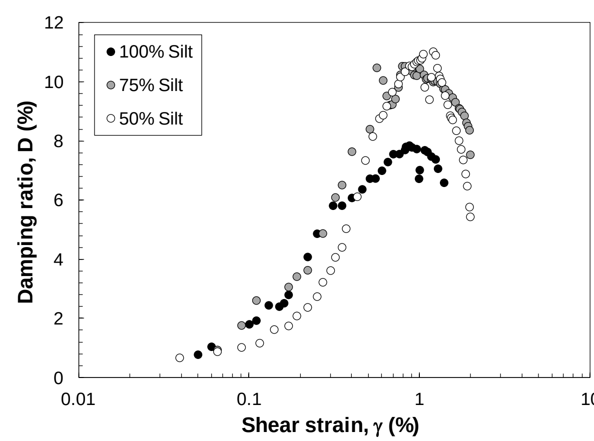

Figure 9: Damping ratios for pure silt and sandy silt specimens at σ'_{vc} = 100 kPa

The decreasing of D at large γ (≥ 1%) would have significant implications on seismic site response by allowing greater amplification of ground motions and subjecting an overlying structure to instances of high horizontal base accelerations.

8 CONCLUSIONS

The elastic and cyclic properties of non-plastic silt and sandy silts (with 75% and 100% silt content) were examined using bender element shear wave velocity measurements and constant-volume cyclic ring shear tests. Shear wave velocity (V_s) measurements were obtained using bender elements at vertical stresses ranging from 50 to 300 kPa, while constant-volume cyclic ring shear tests were carried out to establish undrained shear modulus (G) and damping ratio (D) of silts and sandy silts at large shear strain amplitudes (γ > 0.02%).

The results demonstrated that V_s and the corresponding maximum shear modulus (G_o) significantly decrease with increasing void ratio. It was also found that V_s is a function of the effective overburden stress to the power of 0.31 - 0.34 for silt and sandy silt soils, which is greater than that (0.25) suggested by Robertson et al. (1992). An empirical correlation was calibrated for estimating initial shear modulus of the pure silt and sandy silt specimens and it was found that G_o increased with increasing silt content. Furthermore, the secant shear modulus and damping ratio respectively decreased and increased with shear strains up to about 1%. It was however observed that the damping ratios of the silt and sandy silt specimens decreased at larger shear strain amplitudes (γ > 1%) possibly due to soil dilation or shear banding.

9 ACKNOWLEDGEMENTS

The authors acknowledge and highly appreciate the financial support provided by Western University for the purchasing of a cyclic ring shear equipment (Western University Academic Development Fund, Project No. R4890A05) as well as the financial assistance provided to the first author for pursuing graduate studies.

10 REFERENCES

Alarcon-Guzman, A., Chameau, J. L., Leonards, G. A., and Frost, J. D. (1989). "Shear modulus and cyclic undrained behavior of sands." *Soils and Foundations*, 29(4): 105 - 119.

Andrus, R. D., Stokoe, K. H., II, and Chung, R. M. (1999). "Draft guidelines for evaluating liquefaction resistance using shear wave velocity measurements and simplified procedures." National Institute of Standards and Technology, Gaithersburg, MD.

Assimaki, D., Kausel, E., and Whittle, A. J. (2000). "Model for dynamic shear modulus and damping for granular soils." *Journal of Geotechnical & Geoenvironmental Engineering*, 126(10): 859-869.

ASTM (2006a). "Standard D4253: Standard test methods for maximum index density and unit weight of soils using a vibratory table." *Annual Book of ASTM Standards*, ASTM International, West Conshohocken, PA.

ASTM (2006b). "Standard D4254: Standard test methods for minimum index density and unit weight of soils and calculation of relative density." *Annual Book of ASTM Standards*, ASTM International, West Conshohocken, PA.

ASTM (2006c). "Standard D6467: Standard Test Method for Torsional Ring Shear Test to Determine Drained Residual Shear Strength of Cohesive Soils." *Annual book of ASTM Standards*, ASTM International, West Conshohocken, PA.

ASTM (2007). "Standard D6528: Standard Test Method for Consolidated Undrained Direct Simple Shear Testing of Cohesive Soils." *Annual book of ASTM Standards*, ASTM International, West Conshohocken, PA.

ASTM (2011). "Standard D3999: Standard Test Methods for the Determination of the Modulus and Damping Properties of Soils Using the Cyclic Triaxial Apparatus." *Annual Book of ASTM Standards*, ASTM International, West Conshohocken, PA.

ASTM (2012). "Standards D1557: Standard Test Methods for Laboratory Compaction Characteristics of Soil Using Modified Effort." *Annual Book of ASTM Standards*, ASTM International, West Conshohocken, PA.

Baxter, C. D. P., Bradshaw, A. S., Green, R. A., and Wang, J. H. (2008). "Correlation between cyclic resistance and shear-wave velocity for providence silts." *Journal of Geotechnical and Geoenvironmental Engineering*, 134(1): 37-46.

Bradshaw, A. S., and Baxter, C. D. P. (2007). "Sample preparation of silts for liquefaction testing." *Geotechnical Testing Journal, ASTM*, 30(4): 324 - 332.

Carraro, J. A. H., and Prezzi, M. (2008). "A new slurry-based method of preparation of specimens of sand containing fines." *Geotechnical Testing Journal*, 31(1): 1-11.

Dyvik, R., Berre, T., Lacasse, S., and Raadim, B. (1987). "Comparison of truly undrained and constant volume direct simple shear tests." *Geotechnique*, 37(1): 3 - 10.

El Gamal, A., Yang, Z., Lai, T., Kutter, B. L., and Wilson, D. W. (2005). "Dynamic response of saturated dense sand in laminated centrifuge container." *Journal of Geotechnical and Geoenvironmental Engineering, ASCE*, 131(5): 598 - 609.

El Mohtar, C. S., Drnevich, V. P., Santagata, M., and Bobet, A. (2013). "Combined resonant column and cyclic triaxial tests for measuring undrained shear modulus reduction of sand with plastic fines." *Geotechnical Testing Journal, ASTM*, 36(4): 1 - 9.

El Naggar, M. H. (2003). "Performance evaluation of vibration-sensitive equipment foundation under ground-transmitted excitation." *Canadian Geotechnical Journal*, 40(3): 598 - 615.

El Takch, A. (2013). "Cyclic and post-cyclic response of silt and sandy silt soils." *MESc Thesis*, The University of Western Ontario, London.

Georgiannou, V. N., Hight, D. W., and Burland, J. B. (1991). "Behavior of clayey sands under undrained cyclic triaxial loading." *Geotchnique*, 41: 383 - 393.

Hardin, B. O. (1978). "The nature of stress-strain behavior of soils." *ASCE Geotechnical Engineering Division Speciality Conference on Earthquake Engineering and Soil Dynamics*, Pasadena, California, 3 - 90.

Jamiolkowski, M., Leroueil, S., and Lo Presti, D. C. F. (1991). "Design parameters from theory to practice." *Proceedings of the International Conference on Geotechnical Engineering for Coastal Development: GeoCoast 1991*, Yokohama, Japan, 877 - 917.

Kawaguchi, T., Mitachi, T., and Shibuya, S. (2001). "Evaluation of shear wave travel time in laboratory bender element test." *15th International Conference on Soil Mechanics and Geotechnical Engineering*, Istanbul, 27-31 August 2001, 155 - 158.

Kramer, S. L. (1996). *Geotechnical earthquake engineering*, Prentice Hall, Upper Saddle River, N.J.

Kuerbis, R. H., and Vaid, Y. P. (1988). "Sand sample preparation - the slurry deposition method." *Soils and Foundations*, 28(4): 107 - 118.

La Gatta, D. P. (1970). "Residual strength of clay and clay-shales by rotation shear tests." Harvard University Press, Cambridge, MA.

Ladd, R. S. (1978). "Preparing test specimens using undercompaction." *Geotechnical Testing Journal, ASTM*, 1(1): 16 - 23.

Laird, J. P., and Stokoe, K. H. (1993). "Dynamic properties of remolded and undisturbed soil samples test at high confining pressure." Electric Power Research Institute, Palo Alto, California.

Lanzo, G., Vucetic, M., and Doroudian, M. (1997). "Reduction of shear modulus at small strains in simple shear." *Journal of Geotechnical and Geoenvironmental Engineering, ASCE*, 123(11): 1035 - 1042.

Lee, J., and Santamarina, J. (2005). "Bender elements: performance and signal interpretation." *Journal of Geotechnical and Geoenvironmental Engineering, ASCE*, 131(9): 1063 - 1070.

Lu, N., and Likos, W. J. (2004). *Unsaturated soil mechanics*, Wiley, NewYork.

Lu, N., Wu, B. L., and Tan, C. P. (2007). "Tensile strength characteristics of unsaturated sands." *Journal of Geotechnical and Geoenvironmental Engineering*, 133(2): 144-154.

Matasovic, N., and Vucetic, M. (1993). "Cyclic characterization of liquefiable sands." *Journal of Geotechnical Engineering*, 119(11): 1805 - 1822.

Matasovic, N., and Vucetic, M. (1995). "Seismic response of soil deposits composed of fully-saturated clay and sand layers." *Proc., First International Conference on Earthquake Geotechnical Engineering*, JGS, 611-616.

Mesri, G., and Hayat, T. M. (1993). "The coefficient of earth pressure at rest." *Canadian Geotechnical Journal*, 30: 647 - 666.

Naeini, S. A., and Baziar, M. H. (2004). "Effect of fines content on steady-state strength of mixed and layered samples of a sand." *Soil Dynamics and Earthquake Engineering*, 24(3): 181 - 187.

Richart Jr., F. E., Hall Jr., J. R., and Woods, R. D. (1970). *Vibrations of soils and foundations*, Prentice Hall, Englewood Cliffs, New Jersey.

Robertson, P. K., Woeller, D. J., and Finn, W. D. L. (1992). "Seismic cone penetration test for evaluating liquefaction potential under cyclic loading." *Canadian Geotechnical Journal*, 29(4): 686-695.

Sadrekarimi, A., and Olson, S. M. (2009). "A new ring shear device to measure the large displacement shearing behavior of sands." *Geotechnical Testing Journal, ASTM*, 32(3): 197 - 208.

Sitharam, T. G., Govinda Raju, L., and Srinivasa Murthy, B. R. (2015). "Evaluation of liquefaction potential and dynamic properties of silty sand using cyclic triaxial testing." *Geotechnical Testing Journal, ASTM*, 27(5): 1 - 7.

Stevens, D. K. (2001). "Dynamic site response of dense sand centrifuge models." *MESc Thesis*, University of California, Davis, California.

Vucetic, M. (1986). "Pore pressure buildup and liquefaction of level sandy sites during earthquakes." *PhD Thesis*, Rensselaer Polytechnic Institute, Troy, N.Y.

Vucetic, M., Lanzo, G., and Doroudian, M. (1998). "Damping at small strains in cyclic simple shear test." *Journal of Geotechnical and Geoenvironmental Engineering, ASCE*, 124(7): 585 - 594.

Wang, S., Luna, R., and Stephenson, R. W. (2011). "A slurry consolidation approach to reconstitute low-plasticity silt specimens for laboratory triaxial testing." *Geotechnical Testing Journal, ASTM*, 34(4): 1 - 9.

Wichtmann, T., Navarrete Hernández, M. A., and Triantafyllidis, T. (2015). "On the influence of a non-cohesive fines content on small strain stiffness, modulus degradation and damping of quartz sand." *Soil Dynamics and Earthquake Engineering*, 69: 103 - 114.

Yamamuro, J. A., and Covert, K. M. (2001). "Monotonic and cyclic liquefaction of very loose sands with high silt content." *Journal of Geotechnical and Geoenvironmental Engineering*, 127(4): 314-324.

Youd, T. L., Idriss, I. M., Andrus, R. D., Arango, I., Castro, G., Christian, J. T., Dobry, R., Finn, W. D. L., Harder, L. F., Hynes, M. E., Ishihara, K., Koester, J. P., Liao, S. S. C., Marcuson, W. F., Martin, G. R., Mitchell, J. K., Moriwaki, Y., Power, M. S., Robertson, P. K., Seed, R. B., and Stokoe, K. H. (2001). "Liquefaction resistance of soils: Summary report from the 1996 NCEER and 1998 NCEER/NSF Workshops on Evaluation of Liquefaction Resistance of Soils." *Journal of Geotechnical and Geoenvironmental Engineering*, 127(10): 817-833.

Zhang, J., Andrus, R. D., and Juang, C. H. (2005). "Normalized shear modulus and material damping ratio relationships." *Journal of Geotechnical and Geoenvironmental Engineering, ASCE*, 131(4): 453 - 464.

Zhou, J., Lee, W., and Zhou, K. (1995). "Dynamic properties and liquefaction potential of silts." *International Conference on Earthquake Geotechnical Engineering*, Tokyo, 833 - 838.